Orbital ordering in undoped manganites via a generalized Peierls instability

S. Yarlagadda,[1,2,3] P. B. Littlewood,[3] M. Mitra,[2] and R. K. Monu[1]
[1]*CAMCS, Saha Institute of Nuclear Physics, Calcutta, India*
[2]*TCMP Division, Saha Institute of Nuclear Physics, Calcutta, India*
[3]*Cavendish Laboratory, University of Cambridge, Cambridge CB3 0HE, United Kingdom*
(Received 21 August 2009; revised manuscript received 8 November 2009; published 16 December 2009)

We study the ground-state orbital ordering of $LaMnO_3$, at weak electron-phonon coupling, when the spin state is A-type antiferromagnet. We determine the orbital ordering by extending to our Jahn-Teller system a recently developed Peierls instability framework for the Holstein model [S. Datta and S. Yarlagadda, Phys. Rev. B **75**, 035124 (2007)]. By using two-dimensional dynamic response functions corresponding to a mixed Jahn-Teller mode, we establish that the Q_2 mode determines the orbital order.

DOI: 10.1103/PhysRevB.80.235123 PACS number(s): 71.45.Lr, 71.38.Ht, 75.47.Lx

I. INTRODUCTION

Undoped manganites such as $LaMnO_3$ are the parent systems for the colossal magnetoresistive materials. It is well known that orbital ordering occurs around 780 K resulting in a C-type orbital structure with two kinds of orbitals alternating on adjacent sites in the xy plane while like orbitals are stacked in the z direction.[2] As the temperature is further lowered to 140 K, an A-type spin antiferromagnetic order sets in wherein the spins are ferromagnetically aligned in the xy plane with the spin coupling in the z direction being antiferromagnetic.[3] To explain the observed order several studies have been reported. These studies fall into two broad classes based on the dominant cause for the observed order. One class corresponds to electron-electron (Coulombic) interaction[4–7] being the main cause while the other class treats the cooperative Jahn-Teller (JT) interaction[8–11] as the more important one. Lin and Millis[12] have made a quantitative analysis of the effects of both interactions, generally concluding that both pieces of physics are important, but with many subtleties. There is further controversy about the strength of the electron-phonon interaction with extended x-ray absorption fine structure[13] and pulsed neutron diffraction[14] measurements pointing to strong interaction while some electron microscopy measurements[15,16] have inferred weak coupling in the charge ordered phases. In that regime optical measurements often infer small electronic gaps[17] and measurements of nonlinear transport[18] have been interpreted as due to sliding motion of a density wave.

Without addressing *ab initio* the issues of the quantitative strength of the interactions it is worth understanding how in principle a weak coupling theory might possibly work. The notion of JT is a molecular one, and the linear splitting of levels by a local distortion a useful principle only if the induced gap is much larger than the bandwidth (which it is not). Nonetheless, oxides are generally viewed as a template for strong interaction physics, both of the electronic and phononic variety. In this paper, we step back from the complexities of the full many-body theories to point out that the canonical model for $LaMnO_3$ has a *weak-coupling* generalized Peierls instability that reproduces qualitatively the ordering observed. One advantage of the simplification introduced by our approach is that we can study effects of adiabaticity that turn out to enter *logarithmically* in the ratio of electronic bandwidth to phonon frequency.

Our observation follows straightforwardly from assuming A-type antiferromagnetic ordering. On account of strong Hund's coupling, the transport is restricted to spin polarized electrons in two dimensions only, where, furthermore, the bands are strongly nested. The proximity to a nesting instability allows us to employ the *weak-coupling* framework developed earlier[1,19] and analyze the orbital ordering by using a generalized Peierls instability approach. However, as compared to the one-dimensional Peierls charge density wave (CDW) approach, our higher dimensional orbital density wave (ODW) analysis is more complicated on account of there being two e_g orbitals (with interorbital hopping) and two response functions corresponding to the JT Q_2 and Q_3 distortions. The consequences of a nesting instability on the orbital ordering in $LaMnO_3$ were first discussed by Yarlagadda and Mitra[20] and later qualitatively by Efremov and Khomskii.[21]

In this paper, we study the Peierls instability condition by extending the recently developed reliable condition involving the dynamic susceptibility[1] to a mixed JT mode. We find that Q_2 Jahn-Teller distortion, as observed experimentally, preempts other JT normal mode distortions at all values of adiabaticity and temperature. Furthermore, the condition of instability (i.e., functional dependence of critical coupling on adiabaticity) is qualitatively similar to that of the one-dimensional single-orbital Holstein model. Lastly, we also find that mean-field approximation (in spite of being crude) and static Peierls instability condition (albeit erroneous) indicate that Q_2 mode rather than Q_3 mode determines the orbital order.

II. MODEL HAMILTONIAN

We will now consider manganite systems with two e_g orbitals per site and ignore spin. The Hamiltonian consists of the kinetic term, the ionic term, and the electron-ion interaction term. The kinetic term in momentum space is given by

$$H_1 = \sum_{\vec{p}} \mathbf{B}^{\dagger}_{\vec{p}} \cdot \mathbf{T} \cdot \mathbf{B}_{\vec{p}}, \tag{1}$$

where $\mathbf{B}^{\dagger}_{\vec{p}} \equiv (b^{\dagger}_{1\vec{p}}, b^{\dagger}_{2\vec{p}})$ with b_1 and b_2 corresponding to the destruction operators for electrons with the orthonormal

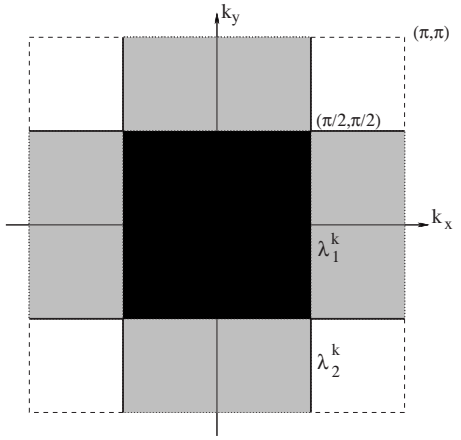

FIG. 1. Fermi seas corresponding to the eigenenergies $\lambda^{\vec{k}}_{1,2}$.

wave functions $\psi_{x^2-y^2}$ and $\psi_{3z^2-r^2}$, respectively. Furthermore, $\mathbf{T}$ is a hermitian matrix with $\mathbf{T}_{1,1}=-1.5t[\cos p_x+\cos p_y]$, $\mathbf{T}_{2,2}=-0.5t[\cos p_x+\cos p_y]$, and $\mathbf{T}_{1,2}=0.5\sqrt{3}t[\cos p_x-\cos p_y]$. The eigenvalues of the kinetic energy are given by

$$\lambda^{\vec{p}}_n = -t[\cos p_x + \cos p_y + (-1)^n\sqrt{\cos^2 p_x + \cos^2 p_y - \cos p_x \cos p_y}]$$

with $n=1,2$. The Fermi sea corresponding to the lower eigenenergy value $\lambda^{\vec{k}}_2$ is given by the union of the region $-\pi/2\le k_x\le\pi/2$ (with all values of k_y allowed) and the region $-\pi/2\le k_y\le\pi/2$ (with all values of k_x allowed) as shown by the shaded region (both dark and light) in Fig. 1. Whereas the Fermi sea corresponding to the higher eigenenergy value $\lambda^{\vec{k}}_1$ is given by the intersection of the region $-\pi/2\le k_x\le\pi/2$ and the region $-\pi/2\le k_y\le\pi/2$, i.e., only the dark shaded region in Fig. 1. Since the number of electrons is equal to the number of sites, the total area occupied by both Fermi seas is equal to the area of the Brillouin zone $(4\pi^2)$. Furthermore, the Fermi surface corresponds to $\lambda^{\vec{k}}_n=0$.

The electron-phonon interaction term is given by

$$H_3 = g\omega_0\sqrt{2M\omega_0}\sum_j [Q_{2j}(b^\dagger_{1j}b_{2j}+b^\dagger_{2j}b_{1j}) + Q_{3j}(b^\dagger_{1j}b_{1j}-b^\dagger_{2j}b_{2j})], \quad (2)$$

while the phononic part of the Hamiltonian is given by

$$H_2 = \omega_0\sum_j\sum_{l=2,3} f^\dagger_{lj}f_{lj}, \quad (3)$$

where $f_{lj}+f^\dagger_{lj}=\sqrt{2M\omega_0}Q_{lj}$. Since we are interested in understanding orbital order, our Hamiltonian does not contain breathing mode distortions.

III. PEIERLS INSTABILITY

In this section, to understand orbital ordering at weak electron-phonon coupling, we consider the Peierls instability condition by using the dynamic susceptibility instead of the static one (see Appendix A for a justification). The cooperative Jahn-Teller effect requires compatible distortions on adjacent sites, which implies that the ordering wave vector in two-dimensions is given by $\vec{Q}\equiv(\pi,\pi)$. We expand the free energy to quadratic order in the relevant degree of freedom (i.e., density n of electrons in an appropriate occupied orbital) as follows:

$$F = \sum_{\vec{q}=\pm\vec{Q}}\left[-\frac{n_{\vec{q}}n_{-\vec{q}}}{2\ \mathrm{Re}\ \chi_\phi(\vec{q},\omega)} + g\omega_0 n_{-\vec{q}}[\langle f^\dagger_{\phi-\vec{q}}\rangle + \langle f_{\phi\vec{q}}\rangle] + \omega_0\langle f^\dagger_{\phi\vec{q}}\rangle\langle f_{\phi\vec{q}}\rangle\right], \quad (4)$$

where $f_{\phi j}+f^\dagger_{\phi j}=\sqrt{2M\omega_0}Q_{\phi j}$. Here, Q_ϕ is the dominant mode defined as $Q_\phi\equiv Q_3\cos(2\phi)+Q_2\sin(2\phi)$ where only orbitals $\psi_{x^2-y^2}\cos(\phi)+\psi_{z^2}\sin(\phi)$ or their orthonormal orbital states $-\psi_{x^2-y^2}\sin(\phi)+\psi_{z^2}\cos(\phi)$ are occupied. The order parameter corresponding to phonons is given by $\langle f_{\phi\vec{Q}}\rangle=|\langle f_{\phi\vec{Q}}\rangle|e^{i\Theta}$. Using reflection symmetry, we first note that $\chi_\phi(\vec{Q},\omega)=\chi_\phi(-\vec{Q},\omega)$, $n_{\vec{Q}}=n_{-\vec{Q}}$, $\langle f_{\phi\vec{Q}}\rangle=\langle f_{\phi-\vec{Q}}\rangle$, and $\langle f^\dagger_{\phi\vec{Q}}\rangle=\langle f^\dagger_{\phi-\vec{Q}}\rangle$. For $g>0$, free energy minimum occurs at $\Theta=\pi$. Minimizing F, with respect to $|\langle f_{\phi\vec{Q}}\rangle|$, yields $|\langle f_{\phi\vec{Q}}\rangle|=gn_{\vec{Q}}$. Thus, we get

$$F = -\left[\frac{1+2g^2\omega_0\ \mathrm{Re}\ \chi_\phi(\vec{Q},\omega)}{\mathrm{Re}\ \chi_\phi(\vec{Q},\omega)}\right]n_{\vec{Q}}n_{-\vec{Q}}. \quad (5)$$

On defining the effective susceptibility as

$$\chi^{eff}_\phi \equiv \frac{\mathrm{Re}\ \chi_\phi}{1+2g^2\omega_0\ \mathrm{Re}\ \chi_\phi}, \quad (6)$$

the Peierls instability condition is given by

$$1+2g^2\omega_0\ \mathrm{Re}\ \chi_\phi(\vec{Q},\omega_0)=0, \quad (7)$$

and leads to the divergence of $\chi^{eff}_\phi(\vec{Q},\omega_0)$. We take $\omega=\omega_0$ in $\chi^{eff}_\phi(\vec{Q},\omega)$ because ω_0 is the natural frequency for lattice distortion. A better explanation for choosing $\omega=\omega_0$ is given in Appendix A.

We need to determine at what value of ϕ one gets the largest value of Re $\chi_\phi(\vec{Q},\omega_0)$. Then one can determine which normal mode gives the lowest value of $g=g_c$ satisfying the Peierls instability condition. Note that, as the rotational angle ϕ (for $0\le\phi\le\pi/2$) is varied, all possible normal modes are spanned starting from Q_3 at $\phi=0$ to Q_2 at $\phi=\pi/4$ and then to $-Q_3$ at $\phi=\pi/2$. The dynamic susceptibility is given by

$$\chi_\phi(\vec{q},\omega)=\sum_n\left[\frac{|\langle n|\rho Q_\phi(\vec{q})|0\rangle|^2}{\omega-\xi_{n0}+i\eta}-\frac{|\langle 0|\rho Q_\phi(\vec{q})|n\rangle|^2}{\omega+\xi_{n0}+i\eta}\right], \quad (8)$$

where

$$\rho Q_\phi(\vec{q}) \equiv \sum_{\vec{k}}[b^\dagger_{1\vec{k}+\vec{q}}b_{1\vec{k}}-b^\dagger_{2\vec{k}+\vec{q}}b_{2\vec{k}}]\cos(2\phi) + [b^\dagger_{1\vec{k}+\vec{q}}b_{2\vec{k}}+b^\dagger_{2\vec{k}+\vec{q}}b_{1\vec{k}}]\sin(2\phi). \quad (9)$$

Then, after some algebra, one gets

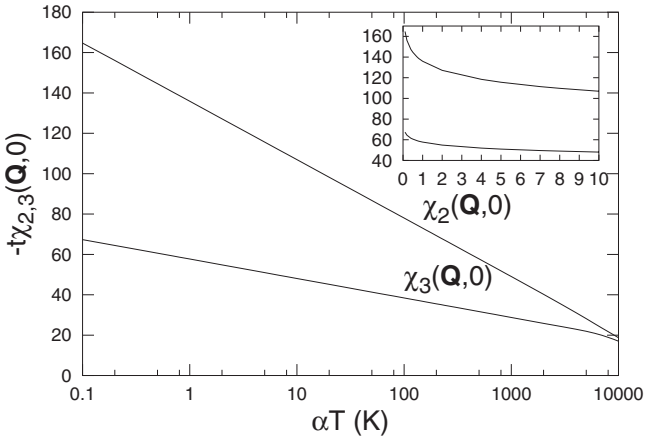

FIG. 2. Plot of $\chi_{2,3}(\vec{Q},0)$ as a function of scaled temperature αT at $\alpha t=1.0$ eV and $\mathbf{Q}\equiv\vec{Q}=(\pi,\pi)$.

$$\mathrm{Re}\ \chi_\phi(\vec{q},\omega_0)=\sum_{\vec{k},\alpha,\beta}\left[\frac{\langle c_{\vec{k}}^{\alpha\dagger}c_{\vec{k}}^{\alpha}\rangle-\langle c_{\vec{k}+\vec{q}}^{\beta\dagger}c_{\vec{k}+\vec{q}}^{\beta}\rangle}{\omega_0+\lambda_\alpha^{\vec{k}}-\lambda_\beta^{\vec{k}+\vec{q}}}\right]\times\cos^2\left[\frac{\theta_{\vec{k}+\vec{q}}+\theta_{\vec{k}}+(\alpha+\beta)\pi}{2}+2\phi\right],\tag{10}$$

where $\alpha=1,2$; $\beta=1,2$; $(c_{\vec{k}}^{1\dagger},c_{\vec{k}}^{2\dagger})=(b_{1\vec{k}}^{\dagger},b_{2\vec{k}}^{\dagger})\cdot\mathbf{M}$, $\mathbf{M}$ is the diagonalizing matrix for the kinetic matrix $\mathbf{T}$ with $\mathbf{M}_{1,1}=\sin(\theta_{\vec{k}}/2)$, $\mathbf{M}_{2,2}=-\sin(\theta_{\vec{k}}/2)$, and $\mathbf{M}_{1,2}=\cos(\theta_{\vec{k}}/2)$. It is interesting to note that, for symmetric wave vectors $\vec{q}=(q,q)$, there is no coupling between the density operators corresponding to Q_2 and Q_3 modes because the interorbital hopping $\mathbf{T}_{1,2}=0.5\sqrt{3}t[\cos p_x-\cos p_y]$ is asymmetric with respect to interchange of momenta p_x and p_y. Thus, for $\vec{q}=(q,q)$, we obtain

$$\chi_\phi(\vec{q},\omega_0)=\chi_3(\vec{q},\omega_0)\cos^2(2\phi)+\chi_2(\vec{q},\omega_0)\sin^2(2\phi),\tag{11}$$

where $\chi_{2,3}$ correspond to JT modes $Q_{2,3}$

A. Static Instability Case

Now, although the static Peierls instability condition $1+2g^2\omega_0\chi_\phi(\vec{Q},0)=0$ erroneously predicts instability even for vanishing values of g, it can still help identify which normal mode produces the Jahn-Teller instability. We will first present results for the static susceptibilities $\chi_{2,3}(\vec{Q},0)$. From the plot of $\chi_{2,3}(\vec{Q},0)$ (shown in Fig. 2) as a function of scaled temperature αT (with α being a scaling parameter and hopping term αt set equal to 1.0 eV) we see that they diverge logarithmically as $T\to 0$ with χ_2 diverging faster than χ_3. At 0 K, both $\chi_2(\vec{Q},0)$ and $\chi_3(\vec{Q},0)$ produce a divergence because of the fact that $\lambda_1^{\vec{k}+\vec{Q}}=-\lambda_2^{\vec{k}}$ and that the Fermi energy is zero. Furthermore, the ratio $\chi_2(\vec{Q},0)/\chi_3(\vec{Q},0)=3$ at 0 K (see Appendix B for details). As can be seen from Fig. 2, $\chi_{2,3}(\vec{Q},0)$ vary logarithmically with k_BT/t for $t/k_BT>2$ and thus have the form

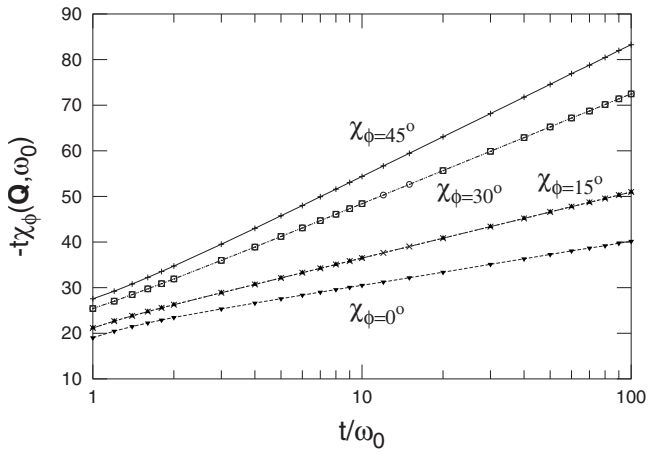

FIG. 3. Plot of Re χ_ϕ as a function of the adiabaticity t/ω_0 for various values of ϕ. $\phi=0°(45°)$ corresponds to $\chi_3(\chi_2)$.

$$\mathrm{Re}[-t\chi_{2,3}(\vec{Q},0)]=m_{2,3}\ln(t/k_BT)+\kappa_{2,3}.\tag{12}$$

We find that $m_2\approx 12.6(m_3\approx 4.2)$ and $\kappa_2\approx 18.3(\kappa_3\approx 18.5)$ with the ratio m_2/m_3 taking the expected value 3. Thus, it appears that Q_2 mode is likely to dictate the orbital ordering.

B. Dynamic Instability Case

While both the static Peierls instability condition and the mean-field energy analysis (see Appendix C) depend only on the polaron size parameter $(g^2\omega_0/t)$, here for the dynamical Peierls instability condition [of Eq. (7)] there are two relevant parameters—namely, adiabaticity parameter t/ω_0 and electron-phonon coupling g. We find that for any value of the adiabaticity parameter t/ω_0 the maximum value of Re $\chi_\phi(\vec{Q},\omega_0)$ occurs at $\phi=\pi/4$, which corresponds to Q_2 mode. In Fig. 3, using Eq. (10), a variation of Re $\chi_\phi(\vec{Q},\omega_0)$ (at 0 K) is plotted for a few representative values of $\phi=0$, $\pi/12$, $\pi/6$, and $\pi/4$. The curves for Re $\chi_{\pi/12}(\vec{Q},\omega_0)$ and Re $\chi_{\pi/6}(\vec{Q},\omega_0)$ (in Fig. 3) verify Eq. (11). Furthermore, we also found numerically that Re $\chi_\phi(\vec{Q},\omega_0)$ [given by Eq. (10)] is symmetric about $\phi=\pi/4$—a fact that follows from Eq. (11).

Quite strikingly, all the Re $\chi_\phi(\vec{Q},\omega_0)$ vary logarithmically with the adiabaticity t/ω_0 for $t/\omega_0>2$ and have the form

$$\mathrm{Re}[-t\chi_\phi(\vec{Q},\omega_0)]=m_\phi\ln(t/\omega_0)+\kappa_\phi.\tag{13}$$

We find that $m_{\pi/4}\approx 12.6(m_0\approx 4.2)$ and $\kappa_{\pi/4}\approx 25.5(\kappa_0\approx 20.9)$. Interestingly, the slopes in Eq. (13) are the same as those in Eq. (12). The ratio of the slopes $m_{\pi/4}/m_0=3$ as expected from the fact that $\chi_2(\vec{Q},0)/\chi_3(\vec{Q},0)=3$ at 0 K. Furthermore, this logarithmic dependence is quite like that for the Holstein model. Using the dynamic Peierls instability condition, similar to the Holstein model case, we are lead to an instability condition of the form $\omega_0=a_1te^{-a_2t/g^2\omega_0}$ where $a_{1,2}$ are constants. We also calculated the critical value of the electron-phonon coupling g_c at which the instability occurs if only Q_2 mode or only Q_3 mode is excited. We find that the value of g_c increases monotonically with the adiabaticity pa-

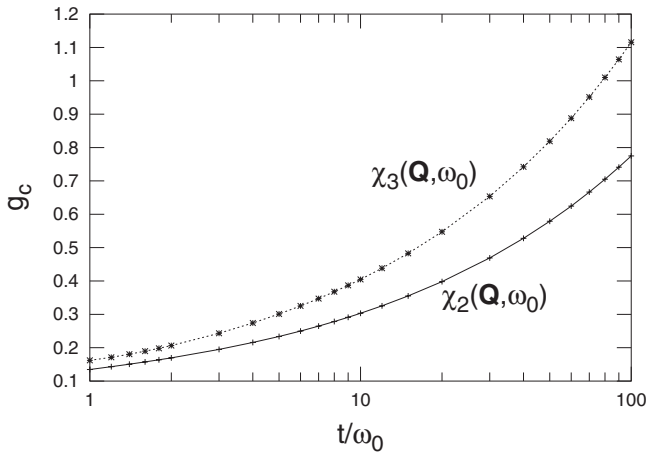

FIG. 4. Plot of the critical coupling g_c as a function of adiabaticity t/ω_0 for the susceptibilities χ_2 and χ_3.

rameter (similar to the Holstein model) and that, as expected, the g_c value is the smallest for Q_2 distortion (as can be seen in Fig. 4) at any value of t/ω_0.

We have also studied the temperature dependence of the dynamical susceptibilities (as shown in Fig. 5) and find that at low temperatures the curves are constant with the extant of the constant region increasing as t/ω_0 decreases. Such a behavior is consistent with the expectation that Re $\chi_\phi(\vec{Q},\omega_0)$ is constant over the region $k_BT \ll \omega_0$. Furthermore, at higher temperatures the susceptibilities for various adiabaticities merge. For instance, when αT attains a value of around 300 K, curves for $t/\omega_0=100$ and ∞ merge (as can be seen from Figs. 2 and 5); and for αT around 2000 K, curves for $t/\omega_0=100$ and 5 merge. The high-temperature behavior too is understandable because one expects the effect of nonzero value of ω_0 to vanish when $k_BT \gg \omega_0$. At the Jahn-Teller orbital ordering temperature of 780 K and for realistic values of both t and ω_0 [i.e., for 0.15 eV$\leq t \leq$0.38 eV (Ref. 22) and for 0.06 eV$\leq \omega_0 \leq$0.07 eV (Ref. 23)], range of the critical coupling [as obtained from Eq. (7) and Fig. 5] is $0.2 \leq g_c \leq 0.28$. For instance, at $T=780$ K, $t=0.2$ eV [and

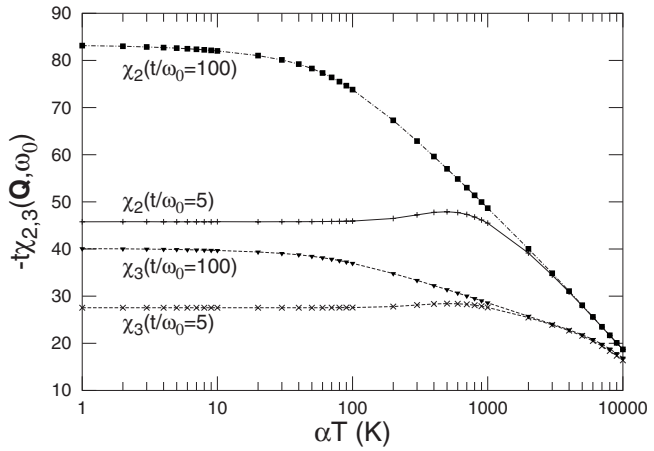

FIG. 5. Plot of the susceptibilities Re $\chi_{2,3}(\vec{Q},\omega_0)$ as a function of the scaled temperature αT for values of scaled hopping αt =1.0 eV and adiabaticity $t/\omega_0=5,100$.

hence, $\alpha=5$ in Fig. 5], and $\omega_0=0.07$ eV, we get $g_c \approx 0.21$. Lastly, for $k_BT \gg \omega_0$ but $k_BT/t<0.5$, the curves display a logarithmic dependence on k_BT/t which is in tune with the logarithmic dependence on ω_0/t of the susceptibility of the Holstein model when $\omega_0/t<0.5$ (see Ref. 1).

IV. CONCLUSIONS

We will now discuss the general features of the orbital-ordering instability and compare it with the Peierls instability in the Holstein model. For the Holstein model, at 0 K, the mean-field approximation gives a gap Δ of the form[24]

$$\Delta = 8te^{-\pi t/g^2\omega_0}. \tag{14}$$

In our case as well, we find that the gap is given by

$$\Delta_{2,3} \approx d^1_{2,3} te^{-d^2_{2,3}t/g^2\omega_0}, \tag{15}$$

where $d^{1,2}_{2,3}$ are constants and $\Delta_{2,3} \approx g^2\omega_0|c_{2,3}|$ with $c_{2,3}$ being amplitudes of orbital density waves defined in Appendix C. It should however be noted that, when $\Delta/\omega_0 \ll 1$, mean-field gives erroneous results. For instance, it predicts a gap even when the electron-phonon coupling g is small. Although, mean-field approximation is inaccurate at the transition, it can still help us figure out which of the two JT modes is dominant. As shown in Appendix C, mean-field correctly shows that Q_2 mode prevails over Q_3 mode.

Next, in the Holstein model,[1,25] at 0 K and $t/\omega_0>2$, the actual instability condition is given by

$$\omega_0 = 8te^{-\pi t/g^2\omega_0}. \tag{16}$$

For our JT system too, at $k_BT \ll \omega_0$ and $(k_BT \gg \omega_0)$ and when $t/\omega_0>2(t/k_BT>2)$, the instability is of the form

$$\omega_0(\gamma k_BT) = a_1te^{-a_2t/g^2\omega_0}, \tag{17}$$

and thus, such as the Holstein model, has an essential singularity at $g=0$. We also note that one cannot get the correct Peierls instability condition by the approximation $P^2_\phi/(2M) + KQ^2_\phi/2 \approx KQ^2_\phi/2$ for the normal mode distortion even when t/ω_0 is large. This is because, when $P^2_\phi/(2M)=0$, the double commutator for the distortion Q_ϕ becomes zero,

$$\ddot{Q}_{\phi\vec{Q}} = -[[Q_{\phi\vec{Q}},H],H] = 0, \tag{18}$$

which implies that phase transition always occurs!

In summary, we observe that owing to the one-dimensional like Fermi surface at zero doping in manganites (as shown in Fig. 1), there are strong similarities of the above mentioned nature between our JT system and the one-dimensional Holstein model. The one-dimensionality of our manganite system is a result of the flatness of the Fermi surface [as can be seen, for instance, from Eq. (B7)]. When $t/[\max\{\omega_0,k_BT,\Delta_\phi\}]>2$, we find that the susceptibility Re$[-t\chi_\phi(\vec{Q},\omega_0)]$ varies logarithmically with respect to $t/[\max\{\omega_0,k_BT,\Delta_\phi\}]$ and has the general form

$$\mathrm{Re}[-t\chi_\phi(\vec{Q},\omega_0)] = m_\phi \ln(t/[\max\{\omega_0,\gamma k_BT,\Delta_\phi\}]) + \kappa_\phi,$$

with $\gamma \approx 1.77$ and both m_ϕ and κ_ϕ being given by Eq. (13). Using this logarithmic relation and the generalized Peierls

instability condition of Eq. (7), one obtains the explicit form of the instability condition.

In conclusion, we have studied orbital ordering for the ground state of the undoped manganite systems in the weak electron-phonon coupling regime $g\omega_0/t<1$. We employ the generalized dynamic Peierls instability condition $1+2g^2\omega_0$ Re $\chi_\phi(\vec{Q},\omega_0)=0$ to figure out which normal mode or combination of normal modes causes the instability. It is also important to note that the dynamic Peierls instability condition does not suffer from the problem of predicting CDW instability at vanishingly small electron-phonon coupling (i.e., $g\to 0$) as does the usual static Peierls instability condition $[1+2g^2\omega_0\chi_\phi(\vec{Q},0)=0]$. We find that Q_2 Jahn-Teller distortion produces the first instability and thus pre-empts other normal mode distortions. Thus the two-dimensional orbital ordering, in the ferromagnetic planes of the observed A-type antiferromagnetic state, is governed by the Q_2 JT mode being cooperatively excited in the system. Hence, we find that the experimentally observed order can be explained even without considering electron-electron interactions.

Before we close, a few general discussions are in order. Above the magnetic transition temperature T_N, where orbital structure does not change much, transport is permitted in the third direction and the Fermi surface for three dimensions should be considered. Then, although the bands are not flat, we still have the nesting condition $\lambda_1^{\vec{k}+\vec{Q}}=-\lambda_2^{\vec{k}}$ for $\vec{Q}=(\pi,\pi,\pi)$ and hence the static susceptibilities will diverge. However, the experimental ordering wave vector is $(\pi,\pi,0)$ and not (π,π,π). To get the observed ordering one will have to incorporate additional physics such as octahedral tilting. Next, at nonzero temperatures below T_N, hopping in the third direction is small but nonzero owing to the nonsaturation in A-type antiferromagnetic order. Then flatness (one-dimensionality) of the Fermi surface would be lost. However, hopping in the third direction increases with temperature and the situation is different from that mentioned in Ref. 26 where, since the hopping in the transverse direction decreases with increasing temperature, re-entrant behavior could occur. Lastly, electron-electron interactions can have an effect on the nesting conditions as pointed out by Kugel, Sboychakov, and Khomskii.[27] These authors find that electron-electron interactions lead to the occurrence of nesting at a density of less than an electron per site. However, in this work, Luttinger's theorem is violated [see Fig. 5(e) in Ref. 27 and implications of that should be investigated for non-Fermi liquid behavior. If, indeed in a full-fledged calculation, beyond the Hubbard I approximation, nesting (with flat Fermi surface) occurs at a lower density, then a corresponding ODW instability condition should be reanalyzed for such a situation.

ACKNOWLEDGMENTS

One of the authors (S.Y.) would like to thank S. Datta and R. Ramakumar for useful discussions. This work was partially funded by UKIERI and CAMCS of SINP.

APPENDIX A: JUSTIFICATION FOR DYNAMIC PEIERLS INSTABILITY CONDITION

We shall give a heuristic justification for the use of dynamic susceptibility in the Peierls instability condition

$$1+2g^2\omega_0 \text{ Re } \chi_\phi(\vec{Q},\omega_0)=0. \tag{A1}$$

Let $Q_{\phi\vec{Q}}$ be the dominant normal mode distortion operator (at wave vector $\vec{Q}$) in the Fourier transformed space. We know that the double time derivative of the operator $Q_{\phi\vec{Q}}$ is given by

$$\ddot{Q}_{\phi\vec{Q}}=-[[Q_{\phi\vec{Q}},H],H]. \tag{A2}$$

Then on taking matrix elements we get

$$\langle\Phi_1|\ddot{Q}_{\phi\vec{Q}}|\Phi_0\rangle=-(E_{\Phi_1}-E_{\Phi_0})^2\langle\Phi_1|Q_{\phi\vec{Q}}|\Phi_0\rangle, \tag{A3}$$

where Φ_n is an eigenstate with n phonons all of which are in the state $\vec{Q}$. When $\omega_{eff}^2\equiv(E_{\Phi_1}-E_{\Phi_0})^2\le 0$, instability occurs for transition from $|\Phi_0\rangle$ to $|\Phi_1\rangle$ provided that $\langle\Phi_1|Q_{\phi\vec{Q}}|\Phi_0\rangle\neq 0$. Now, at weak electron-phonon couplings (i.e., when $g\omega_0/t<1$)

$$E_{\Phi_1}-E_{\Phi_0}=\omega_0+\text{Re }\Sigma_\phi(\vec{Q},\omega_0)=\omega_0+g^2\omega_0^2 \text{ Re } \chi_\phi(\vec{Q},\omega_0), \tag{A4}$$

where Σ_ϕ is the self-energy corresponding to mode $Q_{\phi\vec{Q}}$. Thus, when

$$\omega_{eff}^2=\omega_0^2[1+2g^2\omega_0 \text{ Re } \chi_\phi(\vec{Q},\omega_0)]=0, \tag{A5}$$

CDW instability occurs. The above instability condition is exact up to second-order in perturbation theory. A more detailed and rigorous derivation of the dynamic Peierls instability condition is given in Ref. 1.

APPENDIX B: RATIO OF STATIC JT SUSCEPTIBILITIES

We will show analytically that $\chi_2(\vec{Q},0)/\chi_3(\vec{Q},0)=3$ at 0 K. Understanding the susceptibilities is complicated because the eigenstates [corresponding to the eigenvalues $\lambda_{1,2}^{\vec{k}}$] are a linear combination of the states ψ_{k,x^2-y^2} and $\psi_{k,3z^2-r^2}$ with coefficients that are a function of the wave vector $\vec{k}$. More precisely, the eigenvectors for $\lambda_{1,2}^{\vec{k}}$ are given by $(c_{\vec{k}}^{1\dagger},c_{\vec{k}}^{2\dagger})=(b_{1\vec{k}}^\dagger,b_{2\vec{k}}^\dagger)\cdot\mathbf{M}$, where $\mathbf{M}$ is the diagonalizing matrix for the kinetic matrix $\mathbf{T}$ with $\mathbf{M}_{1,1}=\sin(\theta_{\vec{k}}/2)$, $\mathbf{M}_{2,2}=-\sin(\theta_{\vec{k}}/2)$, and $\mathbf{M}_{1,2}=\cos(\theta_{\vec{k}}/2)$.

Now, from the kinetic matrix $\mathbf{T}$, we get

$$\cos(\theta_{\vec{p}})=\frac{0.5[\cos p_x+\cos p_y]}{\sqrt{\cos^2 p_x+\cos^2 p_y-\cos p_x\cos p_y}}, \tag{B1}$$

and

$$\sin(\theta_{\vec{p}})=\frac{0.5\sqrt{3}[\cos p_x-\cos p_y]}{\sqrt{\cos^2 p_x+\cos^2 p_y-\cos p_x\cos p_y}}. \tag{B2}$$

In the expressions for $\chi_{2,3}(\vec{Q},0)$ given below

$$\chi_2(\vec{Q},0) = \sum_{\vec{k},\alpha,\beta} \left[\frac{\langle c_{\vec{k}}^{\alpha\dagger} c_{\vec{k}}^{\alpha} \rangle - \langle c_{\vec{k}+\vec{Q}}^{\beta\dagger} c_{\vec{k}+\vec{Q}}^{\beta} \rangle}{\lambda_{\alpha}^{\vec{k}} - \lambda_{\beta}^{\vec{k}+\vec{Q}}} \right] \times \sin^2 \left[\frac{\theta_{\vec{k}+\vec{Q}} + \theta_{\vec{k}} + (\alpha+\beta)\pi}{2} \right], \quad \text{(B3)}$$

and

$$\chi_3(\vec{Q},0) = \sum_{\vec{k},\alpha,\beta} \left[\frac{\langle c_{\vec{k}}^{\alpha\dagger} c_{\vec{k}}^{\alpha} \rangle - \langle c_{\vec{k}+\vec{Q}}^{\beta\dagger} c_{\vec{k}+\vec{Q}}^{\beta} \rangle}{\lambda_{\alpha}^{\vec{k}} - \lambda_{\beta}^{\vec{k}+\vec{Q}}} \right] \times \cos^2 \left[\frac{\theta_{\vec{k}+\vec{Q}} + \theta_{\vec{k}} + (\alpha+\beta)\pi}{2} \right], \quad \text{(B4)}$$

because $\lambda_2^{\vec{k}+\vec{Q}} = -\lambda_1^{\vec{k}}$ and since on the Fermi surface (FS) $\lambda_1^{\vec{k}} = 0$, the following term diverges

$$\left[\frac{\langle c_{\vec{k}}^{1\dagger} c_{\vec{k}}^{1} \rangle - \langle c_{\vec{k}+\vec{Q}}^{2\dagger} c_{\vec{k}+\vec{Q}}^{2} \rangle}{\lambda_1^{\vec{k}} - \lambda_2^{\vec{k}+\vec{Q}}} \right]. \quad \text{(B5)}$$

Furthermore, because $\lambda_1^{\vec{k}+\vec{Q}} = -\lambda_2^{\vec{k}}$ and since $\lambda_2^{\vec{k}} = 0$ on the FS, the following term also diverges

$$\left[\frac{\langle c_{\vec{k}}^{2\dagger} c_{\vec{k}}^{2} \rangle - \langle c_{\vec{k}+\vec{Q}}^{1\dagger} c_{\vec{k}+\vec{Q}}^{1} \rangle}{\lambda_2^{\vec{k}} - \lambda_1^{\vec{k}+\vec{Q}}} \right]. \quad \text{(B6)}$$

Then

$$\chi_2(\vec{Q},0)/\chi_3(\vec{Q},0) = \frac{\cos^2 \left[\frac{\theta_{\vec{k}+\vec{Q}} + \theta_{\vec{k}}}{2} \right]_{FS}}{\sin^2 \left[\frac{\theta_{\vec{k}+\vec{Q}} + \theta_{\vec{k}}}{2} \right]_{FS}} = \frac{\sin^2(\theta_{\vec{k}})_{FS}}{\cos^2(\theta_{\vec{k}})_{FS}} = 3, \quad \text{(B7)}$$

where use has been made of the fact that the FS is flat and one-dimensional like and that on the FS either $k_x = \pm \pi/2$ or $k_y = \pm \pi/2$.

APPENDIX C: MEAN-FIELD CDW ANALYSIS

Assuming that the total wave function of the system is separable into a phononic part and an electronic part, after averaging the Hamiltonian over the phononic coordinates, we get the following effective Hamiltonian (with details given in Ref. 19):

$$\bar{H} = \sum_{\vec{p}} \mathbf{B}_{\vec{p}}^{\dagger} \cdot \mathbf{T} \cdot \mathbf{B}_{\vec{p}} - 2g^2\omega_0 \sum_j [(b_{1j}^{\dagger} b_{2j} + b_{2j}^{\dagger} b_{1j}) \times \langle b_{1j}^{\dagger} b_{2j} + b_{2j}^{\dagger} b_{1j} \rangle + (b_{1j}^{\dagger} b_{1j} - b_{2j}^{\dagger} b_{2j}) \langle b_{1j}^{\dagger} b_{1j} - b_{2j}^{\dagger} b_{2j} \rangle] + g^2\omega_0 \sum_j \langle b_{1j}^{\dagger} b_{2j} + b_{2j}^{\dagger} b_{1j} \rangle^2 + \langle b_{1j}^{\dagger} b_{1j} - b_{2j}^{\dagger} b_{2j} \rangle^2, \quad \text{(C1)}$$

where $\langle .. \rangle$ implies averaging over the relevant coordinates which here are electronic.

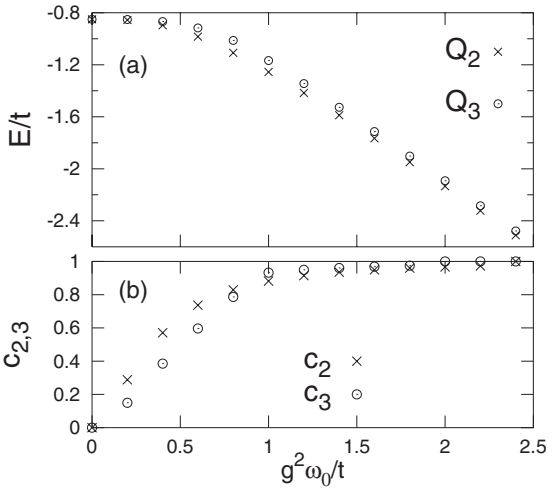

FIG. 6. (a) Dependence of dimensionless ground state energy per site (E/t) on dimensionless polaronic energy $(g^2\omega_0/t)$ for cooperative Q_2 and Q_3 modes; (b) variation of coefficients $c_{2,3}$ of ODW order parameters for Q_2 and Q_3 distortions as a function of $g^2\omega_0/t$.

Based on the arguments that wave vector $\vec{Q}$ determines the orbital ordering in two-dimensions (as discussed in Sec. III), we compute the ground-state energy using mean-field when only either Q_2 mode or Q_3 mode gets excited cooperatively in the system. The order parameters are given by $\langle b_{1j}^{\dagger} b_{2j} + b_{2j}^{\dagger} b_{1j} \rangle = c_2 \cos(\vec{Q} \cdot \vec{R}_j)$ and $\langle b_{1j}^{\dagger} b_{1j} - b_{2j}^{\dagger} b_{2j} \rangle = c_3 \cos(\vec{Q} \cdot \vec{R}_j)$ with $-1 \le c_{2,3} \le 1$ and $\vec{R}_j$ being the position vector. Here, it should be pointed out that the order parameter $\langle b_{1j}^{\dagger} b_{2j} + b_{2j}^{\dagger} b_{1j} \rangle$ corresponds to the density difference of electrons in the two orbitals $\psi_X \equiv (\psi_{x^2-y^2} - \psi_{3z^2-r^2})/\sqrt{2}$ and $\psi_Y \equiv -(\psi_{x^2-y^2} + \psi_{3z^2-r^2})/\sqrt{2}$ (as described in Ref. 10).

The unit cell needed to compute the ground-state energy consists of two adjacent sites with the Brillouin zone being given by $-\pi \le (k_x + k_y) \le \pi$ and $-\pi \le (k_x - k_y) \le \pi$. We diagonalize a 4×4 matrix at each momentum and integrate the lowest two eigenenergies over the Brillouin zone to obtain the ground state energy. The results of our calculations are shown in Fig. 6. From Fig. 6(a), we see that the ground state energy corresponds to the Q_2 mode with the difference in energy between the Q_2 only state and the Q_3 only state peaking at intermediate values of the dimensionless polaronic energy $(g^2\omega_0/t)$. For zero values and infinite values of the polaronic energy both modes yield the same energy because zero value implies no phononic coupling effect while infinite value corresponds to localized polarons. Thus for large values of the polaronic energy, the ground state energy is only slightly smaller than the polaronic energy. Furthermore, from Fig. 6(b) we also see that, as the polaronic energy increases, the values of $c_{2,3}$ increase and become unity around $g^2\omega_0/t \sim 2$ implying that for the $Q_3(Q_2)$ mode $\psi_{x^2-y^2}(\psi_X)$ orbital is occupied fully at one site with the $\psi_{3z^2-r^2}(\psi_Y)$ orbital being fully occupied at the adjacent sites.

[1] S. Datta and S. Yarlagadda, Phys. Rev. B **75**, 035124 (2007).
[2] Y. Murakami, J. P. Hill, D. Gibbs, M. Blume, I. Koyama, M. Tanaka, H. Kawata, T. Arima, Y. Tokura, K. Hirota, and Y. Endoh, Phys. Rev. Lett. **81**, 582 (1998).
[3] E. O. Wollan and W. C. Koehler, Phys. Rev. **100**, 545 (1955).
[4] K. I. Kugel and D. I. Khomskii, Sov. Phys. JETP **37**, 725 (1973).
[5] S. Ishihara, J. Inoue, and S. Maekawa, Phys. Rev. B **55**, 8280 (1997).
[6] L. Sheng and D. N. Sheng, Int. J. Mod. Phys. B **13**, 1397 (1999).
[7] S. Okamoto, S. Ishihara, and S. Maekawa, Phys. Rev. B **65**, 144403 (2002).
[8] A. J. Millis, Phys. Rev. B **53**, 8434 (1996).
[9] T. Hotta, S. Yunoki, M. Mayr, and E. Dagotto, Phys. Rev. B **60**, R15009 (1999).
[10] P. B. Allen and V. Perebeinos, Phys. Rev. B **60**, 10747 (1999).
[11] Z. Popovic and S. Satpathy, Phys. Rev. Lett. **84**, 1603 (2000).
[12] C. Lin and A. J. Millis, Phys. Rev. B **78**, 174419 (2008).
[13] A. Lanzara, N. L. Saini, M. Brunelli, F. Natali, A. Bianconi, P. G. Radaelli, and S.-W. Cheong, Phys. Rev. Lett. **81**, 878 (1998).
[14] Despina Louca, T. Egami, E. L. Brosha, H. Röder, and A. R. Bishop, Phys. Rev. B **56**, R8475 (1997).
[15] J. C. Loudon, S. Cox, A. J. Williams, J. P. Attfield, P. B. Littlewood, P. A. Midgley, and N. D. Mathur, Phys. Rev. Lett. **94**, 097202 (2005).
[16] S. Cox, E. Rosten, J. C. Chapman, S. Kos, M. J. Calderon, D.-J. Kang, P. B. Littlewood, P. A. Midgley, and N. D. Mathur, Phys. Rev. B **73**, 132401 (2006).
[17] K. H. Kim, S. Lee, T. W. Noh, and S.-W. Cheong, Phys. Rev. Lett. **88**, 167204 (2002).
[18] S. Cox, J. Singleton, R. D. McDonald, A. Migliori, and P. B. Littlewood, Nature Mater. **7**, 25 (2008).
[19] S. Yarlagadda, Int. J. Mod. Phys. B **15**, 3529 (2001).
[20] S. Yarlagadda and M. Mitra, arXiv:cond-mat/0310350 (unpublished).
[21] D. V. Efremov and D. I. Khomskii, Phys. Rev. B **72**, 012402 (2005).
[22] A. E. Bocquet, T. Mizokawa, T. Saitoh, H. Namatame, and A. Fujimori, Phys. Rev. B **46**, 3771 (1992); T. Arima, Y. Tokura, and J. B. Torrance, *ibid.* **48**, 17006 (1993); T. Saitoh, A. E. Bocquet, T. Mizokawa, H. Namatame, A. Fujimori, M. Abbate, Y. Takeda, and M. Takano, *ibid.* **51**, 13942 (1995).
[23] M. N. Iliev, M. V. Abrashev, H.-G. Lee, V. N. Popov, Y. Y. Sun, C. Thomsen, R. L. Meng, and C. W. Chu, Phys. Rev. B **57**, 2872 (1998).
[24] R. H. McKenzie, C. J. Hamer, and D. W. Murray, Phys. Rev. B **53**, 9676 (1996).
[25] R. J. Bursill, R. H. McKenzie, and C. J. Hamer, Phys. Rev. Lett. **80**, 5607 (1998).
[26] J. H. Wei, D. Hou, and X. R. Wang, arXiv:0811.2019 (unpublished).
[27] K. I. Kugel, A. O. Sboychakov, and D. I. Khomskii, J. Supercond. Novel Magn. **22**, 147 (2009).